Secondary Electron Transfer Processes in Membranes of *Heliobacillus mobilis*†

Su Lin, Hung-Cheng Chiou, and Robert E. Blankenship*

Department of Chemistry and Biochemistry, Center for the Study of Early Events in Photosynthesis, Arizona State University, Tempe, Arizona 85287-1604

Received January 31, 1995; Revised Manuscript Received July 24, 1995⊗

ABSTRACT: Picosecond transient absorption difference spectroscopic experiments were performed on membranes of the antenna/reaction center complex of *Heliobacillus mobilis* to study the electron transfer processes. Particular emphasis was placed on the blue spectral region, where the difference spectra of iron−sulfur centers and quinones are significantly different. Spectra were measured at room temperature in the wavelength region from 400 to 470 nm and from 630 to 730 nm. Laser excitation was into the 788 nm Q_y band of the bacteriochlorophyll *g* of the reaction center complex. Global analysis in both wavelength regions reveals three kinetic components. A 25 ps phase originates from the decay of the excited state of antenna to form the primary charge-separated state $P798^+A_0^-$; a 600 ps component is assigned to the electron transfer from the primary electron acceptor A_0 to a secondary electron acceptor; a nondecaying component on the time scale measured represents the formation of the secondary charge-separated state. When the secondary electron acceptors were reduced by adding dithionite at pH 11, the 600 ps component disappeared. Only a 25 ps component and a constant were observed in the 630−730 nm region. The 25 ps component is assigned to the excitation decay in the antenna and the formation of $P798^+A_0^-$, just as in the nonreduced sample. In the reduced sample, the $P798^+A_0^-$ state does not decay on the time scale measured. In the 400−470 nm region, the same kinetic behavior was observed. The absorption difference spectra of the primary and the secondary electron acceptor were constructed from different charge-separated states. The $A_0^- - A_0$ spectrum resembles the spectrum of the same state from photosystem I, which also contains a Chl *a* molecule as the primary electron acceptor. The secondary electron acceptor X has an $X^- - X$ difference spectrum similar to F_x in photosystem I from higher plants. The spectra do not give any evidence in favor of a quinone acceptor in heliobacteria, although they do not rule out the possibility that such an acceptor is present.

Heliobacteria are a group of newly discovered non-oxygen evolving photosynthetic bacteria (Gest & Favinger, 1983; Beer-Romero & Gest, 1987; Madigan, 1992; Madigan & Ormerod, 1995). These organisms contain a very simple photosynthetic apparatus in which antenna and reaction center are organized as a single pigment−protein complex (Trost & Blankenship, 1989; Van de Meent et al., 1990). The major pigment in heliobacteria is bacteriochlorophyll (BChl)[1] *g* (Brockmann & Lipinski, 1983; Michalski et al., 1987). About 35−40 BChl *g* pigments were found per complex associated with a primary electron donor. The primary electron donor is believed to be formed by a dimer of BChl *g* and is named P798 after its Q_y transition peak position at room temperature (Fuller et al., 1985; Nuijs et al., 1985). The primary electron acceptor A_0 is identified as an 8^1-hydroxy chlorophyll (Chl) *a* molecule (Van de Meent et al., 1991). Menaquinones and iron−sulfur centers are also found in the reaction center complex of the heliobacteria (Prince et al., 1985; Brok et al., 1986; Trost & Blankenship, 1989; Hiraishi, 1989; Fischer, 1990; Nitschke et al., 1990; Liebl et al., 1993). However, the understanding of their function in electron transfer in heliobacteria is incomplete.

A number of studies have shown that the reaction center of heliobacteria is similar in many ways to those of the green sulfur bacteria and photosystem I from higher plants (Prince et al., 1985; Nitschke et al., 1990; Büttner et al., 1992; Liebl et al., 1993). They all contain iron−sulfur center clusters as one of the early electron acceptors and are therefore known as the Fe-S type of reaction center (Blankenship, 1992). The electron carriers in this type of reaction center have considerably lower redox potential than those of purple bacteria, green filamentous bacteria and photosystem II in higher plants.

Electron transfer processes in the reaction center of photosystem I have been extensively studied [for recent reviews, see Sétif (1992) and Golbeck (1994)]. The initial charge separation to form the $P700^+A_0^-$ state requires 1−3 ps when the excitation resides on the special pair P700 (Holzwarth et al., 1993; Hastings et al., 1994; Kumazaki et al. 1994). The observed chlorophyll excited state lifetime is longer (25−30 ps), due to the fact that most of the time the excitation resides on one of the antenna pigments instead of the special pair.

The primary electron acceptor A_0 is thought to be a Chl *a* molecule (Golbeck & Bryant, 1991). The absorption difference spectrum associated with the reduction of A_0 obtained

† This work was supported by Grant MCB 9418415 from the National Science Foundation. This is Publication No. 239 from the Arizona State University Center for the Study of Early Events in Photosynthesis.

* To whom correspondence should be addressed.

⊗ Abstract published in *Advance ACS Abstracts,* September 15, 1995.

[1] Abbreviations: *Hc. mobilis, Heliobacillus mobilis*; (B)Chl, (bacterio)chlorophyll; P700, primary electron donor of photosystem I absorbing at 700 nm; P798, primary electron donor of heliobacteria absorbing at 798 nm; A_0, primary electron acceptor in photosystem I; A_1, secondary electron acceptor in photosystem I; F_X, F_A/F_B, iron−sulfur centers that act as secondary electron acceptors in photosystem I.

0006-2960/95/0434-12761$09.00/0

by several groups (Nuijs et al., 1986; Shuvalov et al., 1986; Mathis et al., 1988; Kim et al., 1989; Hastings et al., 1994) shows the characteristics of Chl a^- − Chl *a in vitro* (Fujita et al., 1978).

From A_0, the electron is then transferred to the secondary electron acceptor A_1, which is now generally agreed to be a phylloquinone (Brettel, 1988; Golbeck & Bryant, 1991; Biggins & Mathis, 1988). The process of electron transfer from A_0 to A_1 takes 20−50 ps (Fenton et al., 1979; Shuvalov et al., 1986; Wasielewski et al., 1987; Hastings et al., 1994; Hecks et al., 1994).

The kinetics of the further electron transfer from A_1 to iron−sulfur center F_X are not yet well understood, with half-times reported of 15 ns (Mathis & Sétif, 1988), 25 and 200 ns (Brettel, 1988), and 260 ns (Bock et al., 1989). Recent measurements by Sétif and Brettel (1993) found that the optical difference spectra of the faster and slower phases were not the same, and that more intact preparations exhibited less of the fast phase. Similar conclusions were reached by van der Est et al. (1994) from an EPR study.

The reaction center of heliobacteria consists of a peptide homodimer, instead of the heterodimer found in photosystem I (Liebl et al., 1993). At room temperature, the antenna BChl *g* molecule Q_y transition band is centered at 788 nm. The primary donor P798 and acceptor A_0 absorb at 798 and 670 nm, respectively (Fuller et al., 1985; Nuijs et al., 1985; Smit et al., 1987). Other electron acceptors absorb in the 400 nm region that cannot be distinguished individually in the ground state absorption spectrum. Kinetic measurements have indicated that excitation of the antenna system results in a rapid energy transfer to the primary electron donor P798 and forms the primary charge-separated state $P798^+A_0^-$ consequently. The overall excitation energy transfer and trapping time at room temperature is 25−30 ps (Trost & Blankenship, 1989; Van Noort et al., 1992; Lin et al., 1994). The estimated charge separation time is on the order of 1 ps, assuming the trapping-limited case (Lin et al., 1994). A second electron transfer process has a time constant of 500−800 ps at room temperature (Nuijs et al., 1985; Lin et al., 1994). Experimental observations of this process include an absorbance increase at the shorter wavelength side of the P798 bleaching band and a recovery of the bleaching band at 670 nm, both with a time constant of about 600 ps. The 600 ps kinetic phase was not observed when dithionite was added to the sample, which presumably reduces the secondary electron acceptors (Lin et al., 1994). In this case, $P798^+$ and A_0^- recombine with a time constant of 17 ns (Kleinherenbrink et al., 1991, 1994b).

The chemical identity of the secondary electron acceptor in heliobacteria is still not clear, in particular whether or not a quinone is involved in the electron transfer process as one of the secondary electron acceptors. Photoaccumulation of reduced quinones was observed in the low-temperature EPR measurement by several groups (Brok et al., 1986; Fischer, 1990; Nitschke et al., 1990). Double reduction of a quinone acceptor at about −420 mV was proposed to explain the titration behavior of the millisecond recombination component in the kinetics of $P798^+$, in analogy with the double reduction of the phylloquinone acceptor in photosystem I (Trost et al., 1992). On the other hand, measurement with a preparation in which the menaquinones had been extracted showed that the forward electron transfer to secondary electron acceptors was not impaired, which suggests that menaquinone is not an essential participant in the electron acceptor chain of heliobacteria (Kleinherenbrink et al., 1993).

The kinetics and spectra measured on the millisecond time scale from various chemically treated particles provide evidence that an acceptor analogous to F_X of photosystem I is one of the secondary electron acceptors (Kleinherenbrink et al., 1994a). The kinetic behavior of the purified reaction center of *Hc. mobilis* without F_A/F_B indicated a recombination time constant of 14 ms between $P798^+$ and F_X^- (Trost & Blankenship, 1989). Besides that, the only recombination process that has been observed is between $P798^+$ and A_0^-, which takes 17 ns under reducing conditions (Kleinherenbrink et al., 1991, 1994b). There has not previously been a direct comparison between the spectrum of $P798^+F_X^-$ obtained from millisecond measurements and the spectrum measured following the decay of the $P798^+A_0^-$ state. It is not clear at this point whether the spectrum after the 600 ps decay of $P798^+A_0^-$ represents the same state as the $P798^+F_X^-$ state obtained from the millisecond scale measurement, or whether it might represent the $P798^+A_1^-$ state.

While the A_0 and F_X acceptors in heliobacteria have been reasonably well established, the existence of a quinone acceptor is still very uncertain. We present here a transient absorbance change measurement on a 1 ns time scale in the 400-nm region where both quinone and iron−sulfur centers absorb. The excitation has a broad spectral profile from 780 to 820 nm, which excites the Q_y antenna absorbance band centered at 788 nm. This experiment is a direct observation of the spectral evolution on the time scale of which both the primary and secondary electron transfer processes occur. It provides information about the identification of possible molecular species that correspond to the secondary electron acceptor after the primary acceptor A_0.

MATERIALS AND METHODS

Sample Preparation. Hc. mobilis was grown anaerobically at 37 °C under 500 W of incandescent illumination (Gest & Favinger, 1983). Cells were harvested and washed with 20 mM Tris−5 mM sodium ascorbate, pH 8.0, buffer. Preparation of membranes of *Heliobacillus mobilis* was as described in Lin et al. (1994). All buffers used were thoroughly degassed and stored under nitrogen. Membranes were isolated by sonication and centrifugation, followed by ultracentrifugation of the supernatant liquid (Trost et al., 1992).

For the picosecond spectroscopic measurements, two kinds of sample were used. The normal sample was suspended in a buffer solution with 25 mM Tris, pH 8.0, 20 mM ascorbate, and 100 μM phenazine methosulfate (PMS). The sample under reducing conditions was suspended in the buffer with 100 mM glycine, pH 11.0, 20 mM ascorbate, 100 μM PMS, and 50 mM sodium dithionite. Samples were loaded in a spinning cell with a 2.5 mm path length. A typical optical density of 1.7 at 788 nm was used in the measurement. All experiments were carried out at room temperature.

Laser Experiments. The optical setup for the picosecond absorption difference measurement was essentially the same as described in the previous measurements (Lin et al., 1994) except for the modification of the pump beam. A broadband excitation pulse at wavelengths of 780 nm and longer was generated as follows. A train of 590 nm, 200 fs, 100 μJ, and 540 Hz laser pulses was focused on a 0.5 in. thick

rotating fused silica plate to generate a white light continuum. A RG780 cutoff filter was used to block the light at wavelengths shorter than 780 nm. The long-wavelength part of the continuum was sent through a prism dye amplifier (Santa Ana) with dye LDS 798 (Exciton) which was pumped at 532 nm to be amplified. The probe beam was selected from the white light continuum generated by focusing part of the 590 nm laser beam into a 1 cm water flowing cell. The polarization of the probe beam was set at the magic angle with respect to the polarization of the pump beam.

Data analysis techniques including multiexponential kinetic analysis, global analysis, and generation of decay-associated spectra were carried out as described by Lin et al. (1994).

RESULTS

Picosecond absorbance changes were first measured in the Q_y transition band region around 800 nm as a control. For the power of the excitation used, bleaching with a ΔOD of 0.044 centered at 798 nm was measured 100 ps after the excitation (not shown). Previous experiments have shown that the deexcitation and trapping time of the antenna is 25–30 ps and the formation of the secondary charge-separated state takes place in 600 ps (Nuijs et al., 1985; Smit et al., 1987; Trost & Blankenship, 1989; Van Noort et al., 1992; Lin et al., 1994). Therefore, the spectrum at 100 ps represents mostly the primary charge-separated state $P798^+A_0^-$. For a total optical density of the sample in the measuring cell of 1.75, an absorbance change of 0.044 corresponds to a 2.5% bleaching of the total absorption at 788 nm. An absorbance change of 3.5% was observed using saturating excitation flashes. Our measurement on the femtosecond apparatus shows that the sample was not saturated; however, some singlet–singlet excitation annihilation processes within the antenna system do occur at this excitation intensity. This process is not a serious concern at the longer times (>100 ps) that are the central focus of this paper.

Absorption Changes in the 670 nm Region. Transient absorption difference spectra were measured in the wavelength region from 630 to 730 nm on a 1 ns time scale (with a time resolution of 11 ps per point) under both neutral and strongly reducing redox conditions. Absorption changes recorded at 100 ps and at 1 ns after the laser excitation are shown in Figure 1 with no addition (A) and with addition of dithionite (B). For both samples, a prompt absorption increase due to the excited state absorption of the antenna followed by a fast decay was observed over a broad wavelength region. In addition, bleaching of a band centered at 670 nm grew in. The time-resolved spectrum at 100 ps displays a bleached band at 670 nm superimposed on a broad absorption increase. After about 100 ps, the spectral profile remained unchanged on the time scale measured for the sample under the reducing conditions, while the amplitude of the 670 nm bleaching decreased and shifted to the blue in the untreated sample.

The inset in each panel of Figure 1 shows the kinetic trace measured at 670 nm with the theoretical fit. Global analysis on the untreated sample results in three kinetic components, 27 ps, 500 ps, and a constant. Global analysis obtained from the kinetic data with the dithionite-added sample only shows a fast (22 ps) component and a nondecaying component. These results are consistent with the previous measurements with narrow-band excitation at 800 nm (Lin et al., 1994).

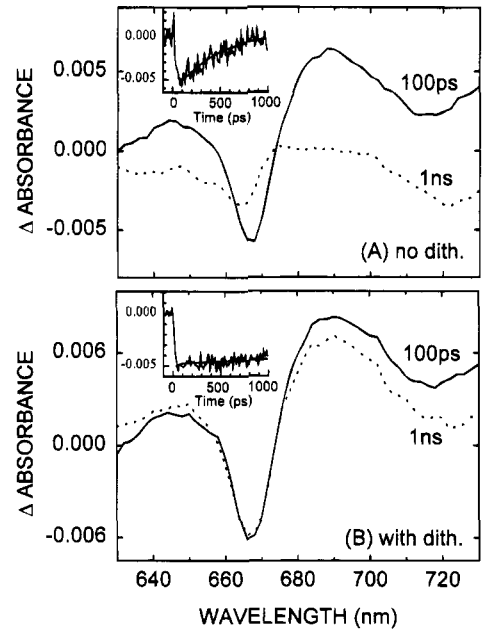

FIGURE 1: Time-resolved absorption difference spectra in the 670 nm region from membranes of *Hc. mobilis* at room temperature taken at 100 ps (solid lines) and at 1 ns (dashed lines). Sample was excited by 200 fs, 540 Hz laser pulses into the 788 nm Q_y transition band. Spectra were obtained from a 11 ps time-resolution scan from the sample (A) under normal conditions and (B) under reducing conditions (50 mM dithionite added at pH 11). Insets show the kinetic traces at 670 nm measured with 11 ps per point over 1 ns time scale. The solid lines are the theoretical fittings from the global analysis over the wavelength region from 630 to 730 nm.

Because the present study utilized a time step of 11 ps, the 20–30 ps time constants are not very accurately determined, and the close correspondence with the time constant for this process determined earlier using higher time resolution may be somewhat fortuitous.

The measurements shown in Figure 1 confirm that the samples were under the desired conditions upon broad-band excitation. The 100 ps spectrum from the normal sample represents the $P798^+A_0^-$ state, and the 1 ns spectrum represents a charge-separated state formed after $P798^+A_0^-$. We name it here the $P798^+X^-$ state. When the secondary electron transfer is blocked by the strongly reducing conditions, the 500 ps phase disappeared. Therefore, only the $P798^+A_0^-$ state is formed which decays with a 17 ns time constant through charge recombination (Kleinherenbrink et al., 1991, 1994b).

Absorption Changes in the Blue Spectral Region. Transient absorption measurements were performed in the wavelength region from 400 to 470 nm on a 1 ns time scale (with a time resolution of 11 ps per point) on the untreated and reduced samples. Figure 2 shows absorption difference spectra taken at 100 ps and 1 ns following the laser excitation (A) with no additions and (B) with addition of dithionite. Spectra in Figure 2A,B were scaled according to the bleaching signal at 798 nm, measured at 100 ps. The 100 ps spectrum from the untreated sample shows a positive band around 455 nm and negative bands at 400 and 420 nm. The zero crossing point is at 438 nm. At 1 ns, the spectrum has shifted to the blue, and the zero crossing point is at 433 nm. The amplitude of both the 450 nm absorption increase and the bleaching decreased. The spectrum measured at 100 ps from the dithionite-added sample has identical features as

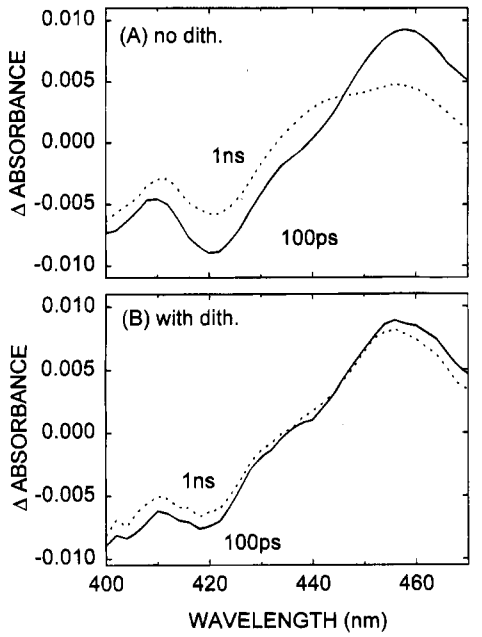

FIGURE 2: Time-resolved absorption difference spectra in the 400 nm region from membranes of *Hc. mobilis* at room temperature taken at 100 ps (solid lines) and at 1 ns (dashed lines) from the normal sample (A) and from the reduced sample (B). Experimental conditions are the same as those in Figure 1.

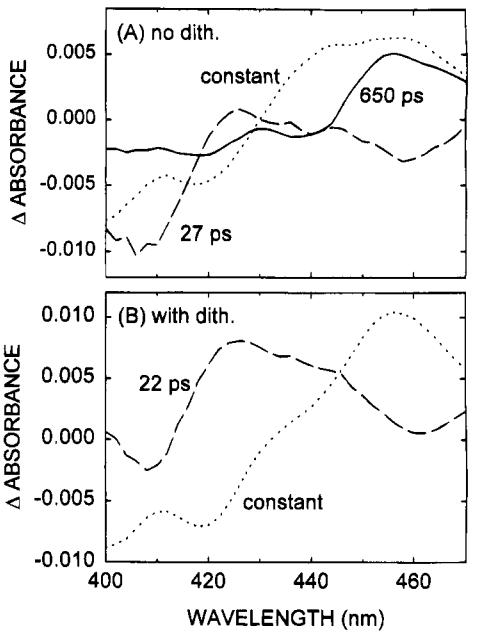

FIGURE 3: Decay-associated spectra of membranes of *Hc. mobilis* in the 400–470 nm region obtained by fitting the absorbance change surface measured on the 1 ns time scale with 11 ps time resolution with (A) the normal sample and (B) the sample under reducing conditions.

the one at 100 ps from the untreated sample. It remains unchanged on the time scale measured. The spectrum at 100 ps from the untreated sample, as well as both the 100 ps and the 1 ns spectra from the reduced sample, represents the absorption differences in the blue region upon formation of $P798^+A_0^-$. The $P798^+A_0^-$ spectrum has very similar features as the one obtained from *Heliobacterium (Hb.) chlorum* on a nanosecond time scale measured by Smit et al. under reducing conditions (Smit et al., 1989).

Global analyses of the entire time/wavelength/ΔOD surface were performed in the wavelength region from 400 to 470 nm. Analysis of the untreated sample results in three kinetic components: 27 ps, 650 ps and a nondecaying component. Global analysis of the dithionite-added sample only gives two components: 22 ps and a nondecaying component. These lifetimes are in good agreement with those obtained in the 670 nm region, although again we note that the conditions of the experiment are such that the 20–30 ps time constant is not very accurately determined. Decay-associated spectra from the fitting of both samples are shown in Figure 3. The fast 20 ps components in both cases have very similar spectral shape. They represent the excitation decay within the antenna system due to both the energy transfer to P798 and the singlet–singlet excitation annihilation. It is also noticed that the two 20–30 ps decay-associated spectra exhibit a base-line shift, which is likely due to the background offset in the fitting. The 650 ps component in the normal sample represents the spectral change from the $P798^+A_0^-$ state to the next charge-separated state $P798^+X^-$. The nondecaying components represent $P798^+A_0^-$ and $P798^+X^-$ from samples with and without dithionite, respectively.

$A_0^- - A_0$ and $X^- - X$ Spectra. Figure 4A illustrates the absorption difference spectra measured from different charge-separated states. The $P798^+A_0^-$ spectrum in Figure 4A was taken from the nondecaying component of the decay-associated spectra from global analysis of the dithionite-added sample (Figure 3B). Comparing with the time-resolved spectrum recorded at 100 ps from the normal sample (Figure 2A, solid line), as well as the 100 ps and 1 ns spectra from the dithionite-added sample (Figure 2B, solid line and dashed line), the overall profiles are almost identical. The $P798^+X^-$ spectrum shown in Figure 4A was the nondecaying component of the decay-associated spectra from global analysis of the untreated sample. It agrees well with the

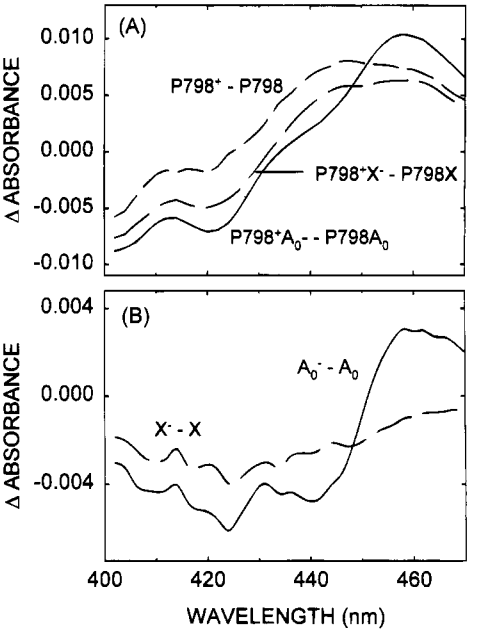

FIGURE 4: (A) Absorption difference spectra representing various charge-separated states: $P7998^+$ (short dashed line), $P798^+A_0^-$ (solid line), and $P798^+X^-$ (long dashed line). The spectra were normalized by comparing absorbance changes at 798 nm. (B) Absorption difference difference spectra constructed from part A: the $A_0^- - A_0$ spectrum (solid line) and the $X^- - X$ spectrum (dashed line).

time-resolved spectrum at 1 ns taken from the untreated sample (Figure 2A, dashed line) except the amplitude of the bleaching around 400 nm is slightly larger than in the time-resolved spectrum. The $P798^+$ spectrum was obtained from millisecond measurements on urea-treated membranes as described by Kleinherenbrink et al. (1994a). In these samples, EPR measurements have shown the absence of the resonance due to $[F_A/F_B]^-$, indicating the loss of activities of F_A/F_B iron−sulfur centers. Vitamin K-3 was also added as an artificial electron acceptor to rapidly reoxidize F_X. Therefore, the absorbance difference spectrum measured at 40 ms after the laser flash represents only the $P798^+$ state. Previous measurements have shown that heliobacteria exhibit transient spectral changes around 780 nm that depend on the redox conditions. However, the bleaching due to $P798^+$ at 798 nm and longer wavelengths remains the same. Therefore, the three spectra shown in Figure 4A were normalized to their $P798^+$ bleaching at 798 nm measured after the primary charge-separated state was formed, and appropriate subtractions were carried out to obtain the difference spectra of the individual components. The largest uncertainties in this method are that different preparations and a different instrument were utilized to obtain the $P798^+ - P798$ difference spectrum than the transient spectra and that the spectra of the individual components are relatively small changes that result from taking the difference of two larger signals.

The $A_0^- - A_0$ spectrum shown as the solid line in Figure 4B was calculated by subtracting the $P798^+$ spectrum from the $P798^+A_0^-$ spectrum. The $A_0^- - A_0$ spectrum exhibits a positive band peaking around 455−460 nm and negative amplitudes at wavelengths shorter than 450 nm. The $X^- - X$ spectrum was constructed by subtracting the $P798^+$ spectrum from the $P798^+X^-$ spectrum and is shown as the dashed line in Figure 4B. This spectrum shows a broad negative band centered around 430 nm.

DISCUSSION

Electron Transfer Kinetics. Previous kinetics measured in the 670 nm region by several groups (Nuijs et al., 1985; Smit et al., 1987; Lin et al., 1994) have shown that only the excited state absorption of the antenna and the primary electron acceptor A_0 contribute in this wavelength region. The kinetic trace at 670 nm shows a prompt absorbance increase due to the excited state absorption from the antenna system followed by a 20−30 ps decay to form a negative bleaching. This bleaching then recovers with a time constant of 600 ps. All of our results are consistent with these earlier studies on the formation and decay of the A_0^- acceptor. The main goal of the present study is to characterize the chemical nature of the acceptor next in line after A_0.

In this measurement, a higher excitation intensity was used in order to observe the absorbance changes of the secondary electron acceptors, for which the absorbance change is known to be very small. Under such strong excitation intensity, singlet−singlet excitation annihilation cannot be avoided within the first few picoseconds. However, due to the time scale used in the experiment, we were not able to resolve it as a separate kinetic component. Therefore, our 20−30 ps decay component in the fitting also contains some contributions from the singlet−singlet annihilation. The 500−650 ps component was clearly resolved and agrees well with the published data. For the sample under reducing conditions, the 500−650 ps decay phase was not observed. This clearly indicates that the electron transfer from A_0 to the secondary electron acceptor was blocked, consistent with results obtained on slower time scales (Kleinherenbrink et al., 1991) and using delayed fluorescence (Kleinherenbrink et al., 1994b).

The picosecond absorption difference measurement technique was extended to the blue region in this work. In this region, the absorption spectrum of heliobacteria is more complicated than that in the 670 nm region. The absorption difference spectrum might include contributions from the ground state absorption of P798, A_0, menaquinone, iron−sulfur centers, and antenna BChl *g* molecules, as well as from various charge-separated states. However, the kinetics measured in the blue spectral region with both the untreated sample and the sample under the reducing conditions closely resemble those measured in the 670 nm region under the corresponding conditions. In the untreated sample, a 20−30 ps component was assigned to the decay of antenna and the formation of the $P798^+A_0^-$ state. The 600 ps component represents the decay of the $P798^+A_0^-$ state and the formation of the next charge-separated state $P798^+X^-$. When the sample was reduced by adding dithionite, only the 20−30 ps and the long-lived components were observed. No additional kinetic component was observed. This clearly indicates that the same kinetic processes were observed in the blue spectral region as at longer wavelengths. The 600 ps phase is the only process observed on this time scale following formation of A_0.

It is worthwhile to compare our results to similar spectroscopic studies of photosystem I. Several kinetic studies have concluded that the secondary electron transfer from A_0 to A_1 is very fast, within a few tens of picoseconds (Shuvalov et al., 1986; Hastings et al., 1994; Hecks et al., 1994). If a similar rapid secondary electron transfer process would occur in heliobacteria, it would be difficult to detect the ground state bleaching at 670 nm associated with the reduction of A_0. This is not the case in heliobacteria because the kinetics at 670 nm clearly show a 25−30 ps formation of the ground state bleaching of A_0 and a 600 ps decay. Because there is no other known or likely electron carrier that absorbs in this region, it is reasonable to make the assignment that the time constant for the formation of the secondary charge-separated state is 600 ps.

The $P798^+A_0^-$ Difference Spectrum. The $P798^+A_0^-$ difference spectrum measured in the blue region was compared with the spectrum thought to represent the same charge-separated state from *Hb. chlorum* measured on the nanosecond time scale (Smit et al., 1987). The latter was measured at 15 ns after a 15 ns laser flash with the sample under reducing conditions. Other studies have shown that under strongly reducing conditions, only the $P798^+A_0^-$ state can be formed and it decays by charge recombination with a time constant of 15−17 ns (Kleinherenbrink et al., 1991, 1994b). Figure 5A shows the $P798^+A_0^-$ spectrum from our measurement obtained from the nondecaying component of the global fitting (Figure 3B) and a point-by-point plot from Smit et al. (1987). The two spectra were scaled without a base-line shift and with the same ratio of positive/negative *y*-axis scale. It can be seen clearly that they are in very good agreement. Both spectra show a positive band peaked around 460 nm and double bleaching bands at 400 and 420 nm.

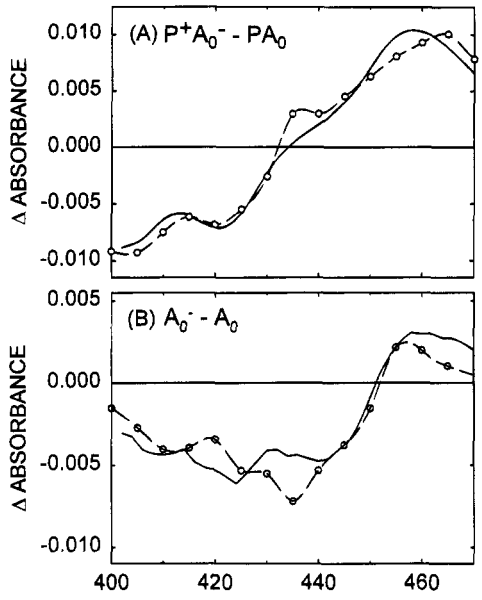

FIGURE 5: (A) Comparison of the $P798^+A_0^-$ spectra obtained from the decay-associated- spectrum of the nondecaying component taken from the sample under reducing conditions (solid line) with published results. The dashed line with open circles is the spectrum representing the same state reconstructed from Smit et al. (1987). The two spectra were scaled by keeping the original base lines and the ratio of the positive/negative range of the *y*-axis the same. (B) Comparison of the $A_0^- - A_0$ spectra of *Hc. mobilis* from Figure 4B (solid line) and that of photosystem I (dashed line) from Mathis et al. (1988). The spectra were scaled in the same way as in panel A.

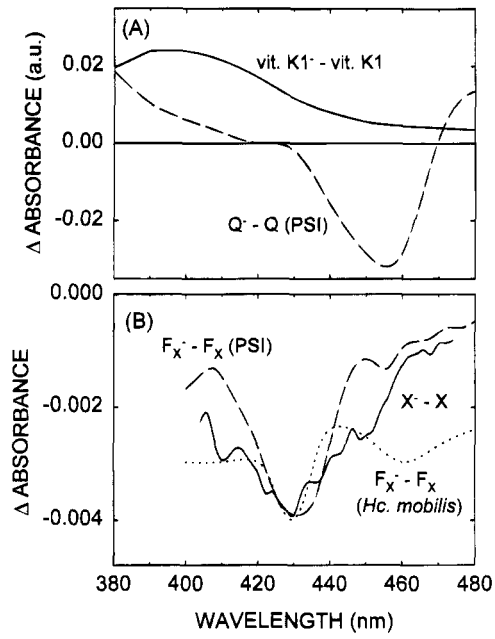

FIGURE 6: (A) Absorption difference spectra of reduced quinone measured from photosystem I (dashed line) and *in vitro* (solid line) from Brettel (1988). (B) Comparison of the $X^- - X$ spectrum (solid line) of *Hc. mobilis* from Figure 4B with published data. The $F_X^- - F_X$ spectrum of photosystem I (dashed line) is from Parrett et al. (1989) and the $F_X^- - F_X$ spectrum of *Hc. mobilis* (dotted line) is from Kleinherenbrink et al. (1994). Spectra were scaled the same way as in Figure 5.

The zero crossing point is around 430 nm.

The $A_0^- - A_0$ and $X^- - X$ spectra. The only published $A_0^- - A_0$ spectrum in the 400 nm wavelength region in this class of reaction centers was measured using the isolated photosystem I core complex devoid of A_1 (Mathis et al., 1988). The $A_0^- - A_0$ spectrum obtained from photosystem I particles was plotted together with the one from *Hc. mobilis* (Figure 4B) in Figure 5B. The $A_0^- - A_0$ spectrum from photosystem I was calculated from the difference spectra of $P700^+A_0^-$ and $P700^+$ by assuming that 80% of the absorbance change at 700 nm is due to the oxidation of P700 species in the normalization (Mathis et al., 1988). The two spectra have very similar features; both have a positive band around 460 nm and zero crossing points around 452 nm. In the 400–450 nm region, they all show negative amplitude. In the 670 nm region, the absorbance changes are not as closely correspondent, as the A_0^- bleaching from photosystem I is centered near 690 nm (Mathis et al., 1988), while the heliobacterial A_0^- is centered at 668 nm. The ratio of the bleaching centered at 670 nm to the absorbance change at 420 nm (measured from the center of the bleached band to a line connecting the positive lobes on the blue and red sides) is 3.2:1, which is close to the ratio of 2.9 measured in the same way from Figure 4 of Mathis et al. (1988).

It is generally accepted that the primary electron acceptor A_0 in photosystem I is a Chl *a* molecule [see Golbeck and Bryant (1991) and Sétif (1992) for reviews]. The primary acceptor of *Hc. mobilis* is thought to be a derivative of a Chl *a* molecule (Van de Meent et al., 1991). The similarity between the two absorbance difference spectra provides further support to the above conclusion.

Is Menaquinone Involved in the Heliobacterial Electron Transfer Chain? The question of the function of quinones as early electron acceptors in all of the FeS-type photosynthetic reaction centers has been a confusing and controversial subject for many years. After a lengthy period of uncertainty, the electron acceptor after A_0 in photosystem I is now generally accepted to be phylloquinone (Biggins & Mathis, 1988). Contradictory results have been reported for the heliobacterial system, as discussed in the introduction. Unfortunately, no information is available on the possible role of quinones in the green sulfur bacterial reaction centers.

The $A_1^- - A_1$ difference spectrum from photosystem I has a positive absorbance change in the near-UV (Brettel, 1988). The $A_1^- - A_1$ spectrum from photosystem I and the vitamin K-1^- − vitamin K-1 spectrum *in vitro* from Brettel (1988) are shown in Figure 6A. The $A_1^- - A_1$ spectrum was obtained from a photosystem I particle of the cyanobacterium *Synechococcus*. A larger uncertainty exists in this spectrum between 410 and 440 nm due to the strong absorbance change of $P700^+$. Nevertheless, all available data indicate that the reduction of a naphthoquinone should cause an absorbance increase in the 400 nm region. However, our $X^- - X$ spectrum shows only negative amplitudes in this wavelength region, and generally much more resembles the spectral characteristics expected for F_X. The $X^- - X$ spectrum was plotted with other $F_X^- - F_X$ spectra obtained from different measurements (Figure 6B). The three spectra were scaled by retaining the original base lines and using the same ratio of positive/negative on the *y*-axes. The dashed line is the $F_X^- - F_X$ spectrum measured from the F_X-containing photosystem I particle of cyanobacteria (Parrett et al., 1989). The dotted line is the $F_X^- - F_X$ spectrum from *Hc. mobilis* obtained from the millisecond absorption difference measurement (Kleinherenbrink et al., 1994a) in which F_A/F_B was removed. Our $X^- - X$ spectrum resembles the $F_X^- - F_X$ spectrum from photosystem I. It also agrees

reasonably well with the millisecond $F_X^- - F_X$ spectrum obtained earlier from *Hc. mobilis*, although the latter spectrum shows an additional bleaching around 460 nm. Reasons for this difference are not yet entirely clear, although we note that our millisecond spectra in this region are somewhat variable. The most important result is that this state clearly shows a bleaching in the 430 nm region, rather than the absorbance increase expected if this state involved a reduced quinone. Taken as a whole, our results indicate that the only charge-separated state observed just after the $P798^+A_0^-$ state is $P798^+F_X^-$.

Our absorption difference spectra measured in the 100 ps to 1 ns time range suggest that the next state observed after $P798^+A_0^-$ represents the $P798^+F_X^-$ state. No $P798^+Q^-$ is detected in this measurement either spectroscopically or kinetically. However, we cannot rule out the possibility of quinone involvement in the electron transfer chain in heliobacteria. If the menaquinone is a mainstream carrier in the electron transfer chain, it could be that it forms with a time constant of 600 ps and decays much faster than 600 ps so that its population in the reduced form never builds up. This situation is reminiscent of the long-standing controversy in purple bacterial reaction centers over the involvement of the accessory bacteriochlorophyll [see Woodbury and Allen (1995) for a review]. This has to be tested using other methods. Other possibilities that cannot be ruled out are that parallel pathways are present or that the menaquinone is a low-efficiency electron acceptor that is not on the main pathway of electron transport but can be reduced under certain conditions.

ACKNOWLEDGMENT

We thank Prof. John Golbeck and Drs. Frank Kleinherenbrink and Paula van Noort for helpful discussions.

REFERENCES

Beer-Romero, P., & Gest, H. (1987) *FEMS Microbiol. Lett. 41,* 109−114.
Biggins, J., & Mathis, P. (1988) *Biochemistry 27,* 1494−1500.
Blankenship, R. E. (1992) *Photosynth. Res. 33,* 91−111.
Bock, C. H., Van de Est, A. J., Brettel, K., & Stehlik, D. (1989) *FEBS Lett. 247,* 91−96.
Brettel, K. (1988) *FEBS Lett. 239,* 93−98.
Brockmann, H. J., & Lipinski, A. (1983) *Arch. Microbiol, 136,* 17−19.
Brok, M., Vasmel, H., Horikx, J. T. G., & Hoff, A. J. (1986) *FEBS Lett. 194,* 322−326.
Büttner, M., Xie, D. L., Nelson, H., Pinther, W., Hauska, G., & Nelson, N. (1992) *Proc. Natl. Acad. Sci. U.S.A. 89,* 8135−8139.
Fenton, J. M., Pellin, M. J., Govindjee, & Kaufmann, K. J. (1979) *FEBS Lett. 100,* 1−4.
Fischer, M. R. (1990) *Biochim. Biophys. Acta 1015,* 471−481.
Fujita, I., Davis, M. S., & Fajer, J. D. (1978) *J. Am. Chem. Soc. 100,* 6280−6282.
Fuller, R. C., Sprague, S. G., Gest, H., & Blankenship, R. E. (1985) *FEBS Lett. 182,* 345−349.
Gest, H., & Favinger, J. L. (1983) *Arch. Microbiol. 136,* 11−16.
Golbeck, J. M. (1994) in *The Molecular Biology of Cyanobacteria* (Bryant, D. A., Ed.) pp 319−360, Kluwer Academic Publishers, Dordrecht, The Netherlands.
Golbeck, J. M., & Bryant, D. A. (1991) *Curr. Top. Bioenerg. 16,* 83−177.
Hastings, G., Kleinherenbrink, F. A. M., Lin, S., McHugh, T., & Blankenship, R. E. (1994) *Biochemistry 33,* 3193−3200.
Hecks, B., Wulf, K., Breton, J., Leibl, W., & Trissl, H.-W. (1994) *Biochemistry 33,* 8619−8624.
Hiraishi, A. (1989) *Arch. Microbiol. 151,* 378−379.
Holzwarth, A. R., Schatz, G., Brock, H., & Bittersmann, E. (1993) *Biophys. J. 64,* 1813−1826.
Kim, D., Yoshihara, K., & Ikegami, I. (1989) *Plant Cell Physiol. 30,* 679−684.
Kleinherenbrink, F. A. M., Aartsma, T. J., & Amesz, J. (1991) *Biochim. Biophys. Acta 1057,* 346−352.
Kleinherenbrink, F. A. M., Ikegami, I., Hiraishi, A., Otte, S. C. M., & Amesz, J. (1993) *Biochim. Biophys. Acta 1142,* 69−73.
Kleinherenbrink, F. A. M., Chiou, H.-C., LoBrutto, R., & Blankenship, R. E. (1994a) *Photosynth. Res. 41,* 115−123.
Kleinherenbrink, F. A. M., Hastings, G., Wittmershaus, B. P., & Blankenship, R. E. (1994b) *Biochemistry 33,* 3096−3105.
Kumazaki, S., Kandori, H., Petek, H., Ikegami, I., Yoshihara, K., & Ikegami, I. (1994) *J. Phys. Chem. 98,* 10335−10342.
Liebl, U., Mockensturm-Wilson, M., Trost, J. T., Brune, D. C., Blankenship, R. E., & Vermaas, W. F. J. (1993) *Proc. Natl. Acad. Sci. U.S.A. 90,* 7124−7128.
Lin, S., Chiou, H.-C., Kleinherenbrink, F. A. M., & Blankenship, R. E. (1994) *Biophys. J. 66,* 437−445.
Madigan, M. T. (1992) in *The Prokaryotes* (Balows, A., Trüper, H. G., Dworkin, M., Schliefer, K. H., & Harder, W., Eds.) 2nd ed., pp 1982−1992, Springer-Verlag, Berlin.
Madigan, M. T., & Ormerod, J. G. (1995) in *Anoxygenic Photosynthetic Bacteria* (Blankenship, R. E., Madigan, M. T., & Bauer, C. E., Eds.) pp 17−30, Kluwer Academic Publishing, Dordrecht, The Netherlands.
Mathis, P., & Sétif, P. (1988) *FEBS Lett. 237,* 65−68.
Mathis, P., Ikegami, I., & Sétif, P. (1988) *Photosynth. Res. 16,* 203−210.
Michalski, T. J., Hunt, J. E., Bowman, M. K., Smith, U., Bardeen, K., Gest, H., Norris, J. R., & Katz, J. J. (1987) *Proc. Natl. Acad. Sci. U.S.A. 84,* 2570−2574.
Nitschke, W., Feiler, U., & Rutherford, A. W. (1990) *Biochemistry 29,* 3834−3842.
Nuijs, A. M., Van Dorssen, R. J., Duysens, L. N. M., & Amesz, J. (1985) *Proc. Natl. Acad. Sci. U.S.A. 82,* 6965−6968.
Nuijs, A. M., Shuvalov, V. A., van Gorkom, H. J., Plijter, J. J., & Duysens, L. N. M. (1986) *Biochim. Biophys. Acta 850,* 310−318.
Parrett, K. G., Mehari, T., Warren, P. G., & Golbeck (1989) *Biochim. Biophys. Acta 973,* 324−332.
Prince, R. C., Gest, H., & Blankenship. R. E. (1985) *Biochim. Biophys. Acta 810,* 377−384.
Sétif, P. (1992) in *Topics in Photosynthesis 11. The Photosystems: Structure, Function and Molecular Biology* (Barber, J., Ed.) pp 471−499, Elsevier Science Publishers, Amsterdam.
Sétif, P., & Brettel, K. (1993) *Biochemistry 32,* 7846−7854.
Shuvalov, V. A., Nuijs, A. M., van Gorkom, H. J., Smit, H. W., & Duysens, L. N. M. (1986) *Biochim. Biophys. Acta 850,* 319−323.
Smit, H. W. J., Amesz, J., & Van de Hoeven, M. F. R. (1987) *Biochim. Biophys. Acta 893,* 232−240.
Smit, H. W. J., van Dorssen, R. J., & Amesz, J. (1989) *Biochim. Biophys. Acta 973,* 212−219.
Trost, J. T., & Blankenship, R. E. (1989) *Biochemistry 28,* 9898−9904.
Trost, J. T., Brune, D. C., & Blankenship, R. E. (1992) *Photosynth. Res. 32,* 11−22.
Van de Meent, E. J., Kleinherenbrink, F. A. M., & Amesz, J. (1990) *Biochim. Biophys. Acta 1015,* 223−230.
Van de Meent, E. J., Kobayashi, M., Erkelens, C., van Veelen, P. A., Amesz, J., & Watanabe, T. (1991) *Biochim. Biophys. Acta 1058,* 356−362.
Van der Est, A., Bock, C., Golbeck, J., Brettel, K., Sétif, P., & Stehlik, D. (1994) *Biochemistry 33,* 11789−11797.
Van Noort, P. I., Gormin, D. A., Aartsma, T. J., & Amesz, J. (1992) *Biochim. Biophys. Acta 1140,* 15−21.
Wasielewski, M. R., Fenton, J. M., & Govindjee (1987) *Photosynth. Res. 12,* 181−190.
Woodbury, N. W., & Allen, J. P. (1995) in *Anoxygenic Photosynthetic Bacteria* (Blankenship, R. E., Madigan, M. T., & Bauer, C. E., Eds.) pp 527−557, Kluwer Academic Publishers, Dordrecht, The Netherlands.

BI950212M